J|A|C|S COMMUNICATIONS

Published on Web 12/22/2009

MCM-22/Silica Selective Flake Nanocomposite Membranes for Hydrogen Separations

Jungkyu Choi and Michael Tsapatsis*

Department of Chemical Engineering and Materials Science, University of Minnesota, Minneapolis, Minnesota 55455

Received October 17, 2009; E-mail: tsapatsi@cems.umn.edu

Zeolite films hold promise as molecular resolution separation membranes with thermal and chemical stability.[1−5] However, the fabrication of all-inorganic molecular sieve films usually includes one or more hydrothermal deposition steps[6,7] which are considered problematic because they are not yet compatible with the cost-effective scale up needed for large scale separation applications.[8] Inspired by a concept proposed earlier[9] and reports on composite zeolite/silica inorganic films fabricated without the need of hydrothermal growth,[10−14] we introduced the preparation of zeolite composite films using layer-by-layer deposition of thin, plate-like crystals of MCM-22.[15] The pore structure of MCM-22[16] includes medium sized pores defined by 10 SiO_4 tetrahedra (10-Member Ring pores: 10MR) along the *a*- and *b*-axes and ultrasmall—potentially H_2-selective—6MR transport limiting apertures along the *c*-axis. Therefore, *c*-out-of-plane oriented MCM-22 films are promising for H_2-separation membranes. MCM-22 has a highly anisotropic plate or disk-like crystal shape, thin along the *c*-crystallographic axis and appropriate for achieving *c*-oriented films. Among the available compositions, a potentially hydrothermally stable one has been reported[17] which could enable H_2-separations in applications like water-gas-shift reactors.

Moreover, MCM-22 can be prepared as ultrathin or even single exfoliated layers preserving the layer structure.[18,19] Thus, it is also a robust model system for exfoliated molecular sieve membranes that can, in principle, be developed using aluminophosphates,[20−22] silicates,[23−26] or other compositions[27,28] as selective flakes. However, only moderate selectivities have been achieved up to now.[15] Here, we show that high performance inorganic molecular sieve membranes based on the concept of selective flakes, eliminating the need for hydrothermal deposition, are feasible.

Membranes were prepared by a certain number of deposition cycles on homemade α-alumina supports. A deposition cycle consisted of MCM-22 particle deposition followed by a silica coating and calcination. Although we envision that MCM-22 particle deposition could be eventually accomplished by a simpler procedure like dip coating, we adopted a robust sonication-assisted method[29] that ensured oriented and compact MCM-22 layers. Surfactant-templated mesoporous silica, selected due to its potential for hydrothermal stability, was deposited by evaporation induced self-assembly (EISA) between MCM-22 particle depositions. Three types of composite membranes were prepared: membranes noted as Ax were made by use of a more dilute EISA silica sol (type A) for x deposition cycles; membranes Bx by use of a more concentrated sol (type B) for x cycles. Membranes noted as AxBy were made by use of type A silica sol for x deposition cycles and by use of type B silica sol for the subsequent y deposition cycles (see Supporting Information).

Figure 1 shows representative Scanning Electron Microscopy (SEM) images and X-ray Diffraction (XRD) data from membranes A3B1 and A3B3. MCM-22 particles are compactly deposited with the basal *ab*-plane parallel to the substrate (Figure 1a) in a film with a thickness approaching 1 μm (Figure 1a inset). The *c*-out-of-plane preferred orientation was verified by XRD patterns (Figure 1b). Membranes with more layers (like A3B3) exhibited more intense peaks, as expected. The rest of the membranes exhibited very similar microstructures to the resolution of SEM (Figure S1) and similar preferred orientation (Figure S2). The film thicknesses are shown in Table S1. Considering the thicknesses of the flakes and films, it appears that the volume fractions of both components are significant.

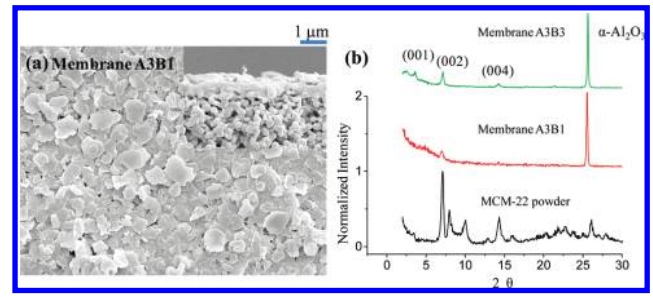

Figure 1. SEM top-view image of membrane A3B1 with cross section shown in the inset (a), and XRD patterns (reflection geometry) of MCM-22 powder (as nonoriented reference) and of membranes A3B1 and A3B3 (b).

Before presenting the single component permeation data for He, H_2, and N_2, it is useful to discuss briefly the expected behavior of the individual components, i.e., MCM-22 and mesoporous silica. The estimated kinetic diameters of He, H_2, and N_2 are 0.26, 0.289, and 0.364 nm, respectively. It is expected that transport through the 6MR limiting aperture will be highly activated but feasible for He and H_2 and not possible for N_2. The activation energy for diffusion of H_2 through the 6 MR of sodalite is reported to be approximately 34 kJ/mol[30] and is comparable to that reported for transport through dense amorphous SiO_2 membranes (35 kJ/mol) and quartz (38 kJ/mol).[31,32] We are not aware of experimental or simulation reports on H_2 diffusion along the *c*-axis of MCM-22, but it is reasonable to expect a similar or higher activation energy as transport is dominated by 6MR crossing. Transport through the 10MR of MCM-22 is expected to be much less activated. A reasonable estimate can be obtained by considering the MFI type zeolite which has 10 MR channels. Indicative activation energies for He, H_2, and N_2 are 8.9, 8.3, and 8.4 kJ/mol, respectively.[33] On the other hand, permeation in the mesoporous silica is expected in the Knudsen regime and, thus, nonactivated with ideal selectivities estimated by the molecular weights of H_2, He, and N_2 to be 3.7 for H_2/N_2 and 1.41 for H_2/He.

The behavior of the composite can be complex and a quantitative analysis requires[34−37] (i) a precise knowledge of permeabilities through the individual components of the composite (silica matrix and MCM-22 flakes) and (ii) a detail description of the microstructure (flake concentration, orientation, and aspect ratio). In addition, the permeation behavior can be affected by the extensive presence of matrix/flake interfaces of unknown structure. Here, we will present the permeation results and qualitatively address the possible contributions.

Figure 2 shows the single component permeances of He, H_2, and N_2 at temperatures ranging from ambient up to 230 °C for

10.1021/ja908864g

membranes A1, A5, B5, A3B2, and A3B3. Good reproducibility is indicated by the data given in Figure S3. Figure 2f shows the H_2/N_2 ideal selectivities from these and other membranes. As expected, permeances decrease and selectivity increases with the number of deposition cycles. The performance of membranes A5 and B5 is quite similar with the H_2/N_2 ideal selectivities approaching 30 at the highest temperatures tested. Even more promising behavior was observed for AxBy type membranes where H_2/N_2 ideal selectivities approached or exceeded 100 and remained high over the range of temperatures studied. The use of silica layers from more dilute sols for the first layers followed by denser silica coatings leads to lower N_2 permeances without affecting the He and H_2 ones. This finding underscores the importance of the matrix material as gap filler and glue in enabling compact film formation and harvesting of the molecular sieving properties of the flakes.

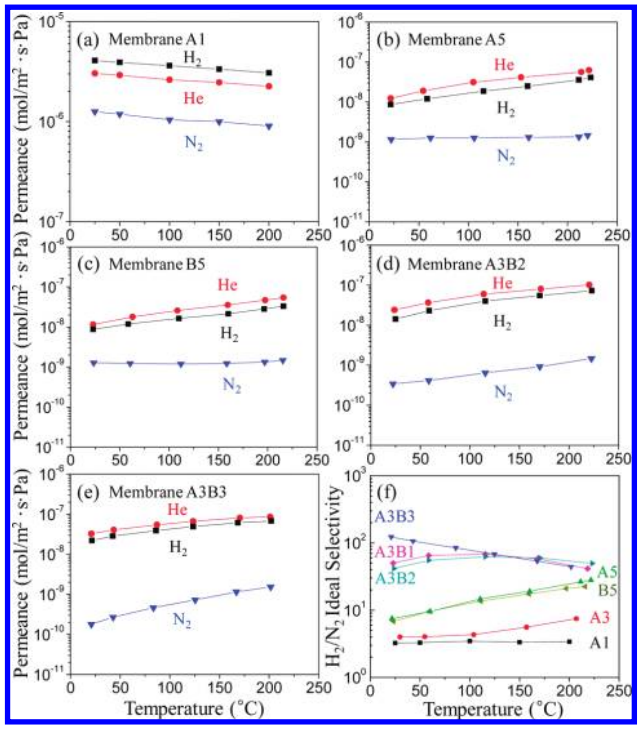

Figure 2. N_2, H_2, and He single gas permeances vs temperature through membranes (a) A1, (b) A5, (c) B5, (d) A3B2, and (e) A3B3. H_2/N_2 ideal selectivities vs temperature through membranes A1, A3, A5, B5, A3B1, A3B2, and A3B3 are shown in (f).

In addition to high H_2/N_2 ideal selectivities, all membranes show selectivity for the smaller He over H_2. Moreover, with the exception of all permeances through membrane A1 and of N_2 permeances for membranes A5 and B5, single gas permeances increase with temperature. All of the above trends exclude Knudsen diffusion as the dominant transport mechanism indicating a certain level of molecular sieving. However, apparent activation energies calculated from the H_2 permeances in the 100−200 °C range are 11.5, 10.1, and 13.7 for membranes A5, B5, and A3B1, respectively. These values are much lower than those expected for permeances controlled exclusively by 6MR transport and somewhat higher than activation energies for 10MR transport. It is unlikely that these differences could be entirely due to adsorption effects, as the heat of adsorption for hydrogen is expected to be low. Therefore, it appears that despite the already attractive membrane performance (Figure S4), there is still considerable room for improving selectivities by reducing the Knudsen and 10MR contributions to gas transport.

Further work could be directed to systematic variations of deposit microstructure (number of layers, concentration and aspect ratio of flakes, control of EISA silica pore structure, etc.) to improve membrane selectivity. Moreover, thinner MCM-22 flakes including single exfoliated layers could be used to improve H_2-permeances. Such thinner flakes would also be desirable from the processing standpoint since they will form more stable suspensions and could be deposited using simpler methods like dip coating. The concept demonstrated here could be attempted for other separations using different flakes with or without a gap filler.

Acknowledgment. Support was provided by DOE (DE-FG26-04NT42119) and in part by NSF through NNIN.

Supporting Information Available: Experimental details; additional SEM, XRD, and permeation data; performance plot. This material is available free of charge via the Internet at http://pubs.acs.org.

References

(1) Davis, M. E. *Nature* **2002**, *417* (6891), 813–821.
(2) Snyder, M. A.; Tsapatsis, M. *Angew. Chem., Int. Ed.* **2007**, *46* (40), 7560–7573.
(3) Caro, J.; Noack, M. *Microporous Mesoporous Mater.* **2008**, *115* (3), 215–233.
(4) Tsapatsis, M. *AIChE J.* **2002**, *48* (4), 654–660.
(5) Tsapatsis, M.; Gavalas, G. R. *MRS Bull.* **1999**, *24* (3), 30–35.
(6) Jeong, H.-K.; Krohn, J.; Sujaoti, K.; Tsapatsis, M. *J. Am. Chem. Soc.* **2002**, *124* (44), 12966–12968.
(7) Lai, Z.; Tsapatsis, M. *Ind. Eng. Chem. Res.* **2004**, *43* (12), 3000–3007.
(8) Koros, W. J.; Mahajan, R. *J. Membr. Sci.* **2000**, *175* (2), 181–196.
(9) Cussler, E. L. *J. Membr. Sci.* **1990**, *52* (3), 275–288.
(10) Farrell, R. A.; Petkov, N.; Amenitsch, H.; Holmes, J. D.; Morris, M. A. *J. Mater. Chem.* **2008**, *18* (19), 2213–2220.
(11) Bein, T.; Brown, K.; Frye, G. C.; Brinker, C. J. *J. Am. Chem. Soc.* **1989**, *111* (19), 7640–7641.
(12) Petkov, N.; Hoelzl, M.; Metzger, T. H.; Mintova, S.; Bein, T. *J. Phys. Chem. B* **2005**, *109* (10), 4485–4491.
(13) Petkov, N.; Mintova, S.; Jean, B.; Metzger, T. H.; Bein, T. *Chem. Mater.* **2003**, *15* (11), 2240–2246.
(14) Seo, T.; Yoshino, T.; Cho, Y.; Hata, N.; Kikkawa, T. *Jpn. J. Appl. Phys., Part 1* **2007**, *46* (9A), 5742–5746.
(15) Choi, J.; Lai, Z.; Ghosh, S.; Beving, D. E.; Yan, Y.; Tsapatsis, M. *Ind. Eng. Chem. Res.* **2007**, *46* (22), 7096–7106.
(16) Leonowicz, M. E.; Lawton, J. A.; Lawton, S. L.; Rubin, M. K. *Science* **1994**, *264* (5167), 1910–1913.
(17) Camblor, M. A.; Corell, C.; Corma, A.; Diaz-Cabanas, M.-J.; Nicolopoulos, S.; Gonzalez-Calbet, J. M.; Vallet-Regi, M. *Chem. Mater.* **1996**, *8* (10), 2415–2417.
(18) Corma, A.; Fornes, V.; Pergher, S. B.; Maesen, T. L. M.; Buglass, J. G. *Nature* **1998**, *396* (6709), 353–356.
(19) Maheshwari, S.; Jordan, E.; Kumar, S.; Bates, F. S.; Penn, R. L.; Shantz, D. F.; Tsapatsis, M. *J. Am. Chem. Soc.* **2008**, *130* (4), 1507–1516.
(20) Jeong, H.-K.; Krych, W.; Ramanan, H.; Nair, S.; Marand, E.; Tsapatsis, M. *Chem. Mater.* **2004**, *16* (20), 3838–3845.
(21) Wang, C.; Hua, W.; Yue, Y.; Gao, Z. *Microporous Mesoporous Mater.* **2007**, *105* (1−2), 149–155.
(22) Wang, J.; Chen, G.; Zhou, Q. *Adv. Compos. Lett.* **2006**, *15* (5), 173–177.
(23) Choi, S.; Coronas, J.; Jordan, E.; Oh, W.; Nair, S.; Onorato, F.; Shantz, D. F.; Tsapatsis, M. *Angew. Chem., Int. Ed.* **2008**, *47* (3), 552–555.
(24) Gorgojo, P.; Uriel, S.; Tellez, C.; Coronas, J. *Microporous Mesoporous Mater.* **2008**, *115* (1−2), 85–92.
(25) Choi, M.; Na, K.; Kim, J.; Sakamoto, Y.; Terasaki, O.; Ryoo, R. *Nature* **2009**, *461* (7261), 246–249.
(26) Jeong, H.-K.; Nair, S.; Vogt, T.; Dickinson, L. C.; Tsapatsis, M. *Nat. Mater.* **2003**, *2* (1), 53–58.
(27) Ding, N.; Kanatzidis, M. G. *Chem. Mater.* **2007**, *19* (16), 3867–3869.
(28) Liu, L.; Ferdov, S.; Coelho, C.; Kong, Y.; Mafra, L.; Li, J. P.; Dong, J. X.; Kolitsch, U.; Sa Ferreira, R. A.; Tillmanns, E.; Rocha, J.; Lin, Z. *Inorg. Chem.* **2009**, *48* (11), 4598–4600.
(29) Lee, J. S.; Ha, K.; Lee, Y.-J.; Yoon, K. B. *Adv. Mater.* **2005**, *17* (7), 837–841.
(30) van den Berg, A. W. C.; Flikkema, E.; Jansen, J. C.; Bromley, S. T. *J. Chem. Phys.* **2005**, *122* (20), 204710/1–204710/6.
(31) Gavalas, G. R.; Megiris, C. E.; Nam, S. W. *Chem. Eng. Sci.* **1989**, *44* (9), 1829–1835.
(32) Tsapatsis, M.; Kim, S.; Nam, S. W.; Gavalas, G. *Ind. Eng. Chem. Res.* **1991**, *30* (9), 2152–2159.
(33) Bakker, W. J. W.; van den Broeke, L. J. P.; Kapteijn, F.; Moulijn, J. A. *AIChE J.* **1997**, *43* (9), 2203–2214.
(34) Guseva, O.; Gusev, A. A. *J. Membr. Sci.* **2008**, *325* (1), 125–129.
(35) Johnson, J. R.; Koros, W. J. *J. Taiwan Inst. Chem. Eng.* **2009**, *40* (3), 268–275.
(36) Pal, R. *J. Colloid Interface Sci.* **2008**, *317* (1), 191–198.
(37) Sheffel, J. A.; Tsapatsis, M. *J. Membr. Sci.* **2007**, *295* (1 + 2), 50–70.

JA908864G